# Coherent control of the electron quantum paths for the generation of single ultrashort attosecond laser pulse

I-Lin Liu,[1,*] Peng-Cheng Li,[1,2,†] and Shih-I Chu[1,3,‡]

[1]*Center for Quantum Science and Engineering, Department of Physics, National Taiwan University, Taipei 10617, Taiwan*

[2]*College of Physics and Electronic Engineering, Northwest Normal University, Lanzhou 730070, China*

[3]*Department of Chemistry, University of Kansas, Lawrence, Kansas 66045, USA*

(Received 6 May 2011; published 15 September 2011)

We report a mechanism and a realizable approach for the coherent control of the generation of an isolated and ultrashort attosecond (as) laser pulse from atoms by optimizing the two-color laser fields with a proper time delay. Optimizing the laser pulse shape allows the control of the electron quantum paths and enables high-harmonic generation from the long- and short-trajectory electrons to be enhanced and split near the cutoff region. In addition, it delays the long-trajectory electron emission time and allows the production of extremely short attosecond pulses in a relatively narrow time duration. As a case study, we show that an isolated 30 as pulse with a bandwidth of 127 eV can be generated directly from the contribution of long-trajectory electrons alone.

DOI: 10.1103/PhysRevA.84.033414 PACS number(s): 32.80.Rm, 42.65.Re

The study of attosecond (as) physics in intense ultrashort laser fields is now a forefront subject of much current interest and significance in science and technology [1,2]. Attosecond pulses can be produced by means of high-harmonic generation (HHG) via atoms in intense laser fields [2,3], and the time profile of the attosecond pulses can be controlled by tuning the carrier-envelope phase [4,5]. Recent progress of attosecond physics includes control of electron wave packets [6], probing of nuclear [7] and electronic dynamics [8], attosecond time-resolved spectroscopy [9], tomographic imaging of molecular orbitals [10], etc. One of the most novel features on the attosecond time scale is the real-time observation of the motion of electrons in atoms and molecules [11,12]. The generation of ever-shorter attosecond pulses has continued to attract much interest and has become one of the most active research directions in attosecond metrology today.

It has been demonstrated experimentally that, by superposing the supercontinuum harmonic spectrum, one can obtain a train of attosecond pulses (ATP) or an isolated pulse of 107 as [13] and 80 as [14]. There are more and more experiments that use two-color lasers to analyze the contribution of the long and short quantum paths of the HHG spectrum [15,16]. Recently, several methods have been proposed for the generation of extremely short attosecond pulse (sub-50 as) and that use two-color laser fields or few-cycle chirped laser pulses. These methods are based on the semiclassical three-step model [17] or the solution of the time-dependent Schrödinger equation (TDSE) of one-dimensional (1D) model systems with a soft potential. However, such short attosecond pulses have not yet been realized experimentally by these methods. In this paper, we present a mechanism and a realizable approach for efficiently generating ultrashort attosecond pulses by controlling the short and long quantum paths by means of optimizing the pulse shape and time delay of two-color laser fields. Our proposed procedure is different from other control methods where only one trajectory is enhanced and the other is suppressed. Our method can enhance the radiation for the two quantum paths and split the radiation near the cutoff region, and short-trajectory electrons are dispersed to different emission times but long-trajectory electrons are confined to a relatively narrower emission-time region. As a result, we can obtain a coherent 30 as pulse due to the contribution of long-trajectory electrons alone. We will also show that such a metrology can be realized experimentally.

HHG xuv attosecond pulses can be studied by solving the following time-dependent Schrödinger equation:

$$i\frac{\partial}{\partial t}\psi(\mathbf{r},t) = \hat{H}\psi(\mathbf{r},t) = [\hat{H}_0 + \hat{V}]\psi(\mathbf{r},t). \tag{1}$$

Here, $\hat{H}_0$ represents unperturbed hydrogen atom Hamiltonian and $\hat{V}$ is the time-dependent atom-field interaction.

The TDSE is solved accurately and efficiently by means of the time-dependent generalized pseudospectral (TDGPS) method [5,18]. The numerical scheme of the TDGPS method consists of two essential steps: (i) The spatial coordinates are optimally discretized in a nonuniform spatial grid by means of the generalized pseudospectral (GPS) technique [18]. This discretization, which uses only a modest number of grid points, is characterized by denser grids near the nuclear origin and sparser grids for larger distances. (ii) A second-order split-operator technique is used in the energy representation which allows the explicit elimination of undesirable fast-oscillating high-energy components for the efficient and accurate time propagation of the wave function:

$$\begin{aligned}\psi(\mathbf{r},t+\Delta t) &\simeq \exp\left(-i\hat{H}_0\frac{\Delta t}{2}\right)\exp\left[-i\hat{V}\left(\mathbf{r},\theta,t+\frac{\Delta t}{2}\right)\Delta t\right] \\ &\quad\times\exp\left(-i\hat{H}_0\frac{\Delta t}{2}\right)\psi(\mathbf{r},t)+O(\Delta t^3).\end{aligned} \tag{2}$$

The TDGPS technique is considerably more efficient and accurate than the conventional time-dependent technique using equal-spacing grid discretization. The unitarity of the wave function is automatically preserved by this procedure and

*r97222060@ntu.edu.tw
†lipc@nwnu.edu.cn
‡sichu@ku.edu

 

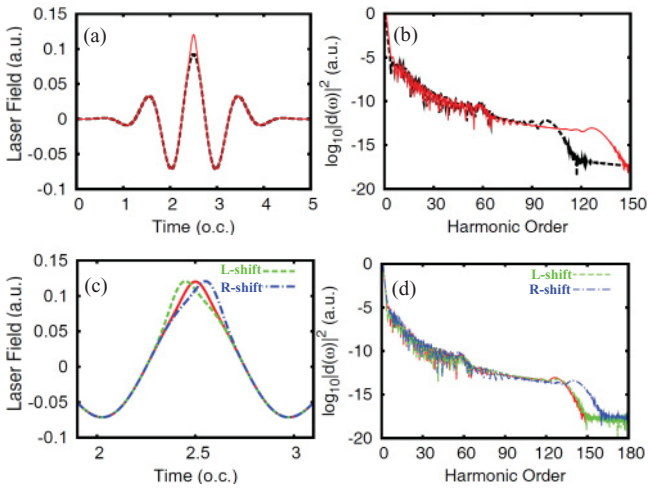


FIG. 1. (Color online) (a) Laser field and (b) corresponding HHG power spectrum from hydrogen atoms driven by a 1064 nm laser pulse (dashed black line) and a 1064 nm laser enhanced in the center part (solid red line). The original 1064 nm laser-field parameters are a peak intensity $I = 3 \times 10^{14}$ W/cm$^2$ and a 3 fs Gaussian pulse envelope. (c) Left-shifted (dotted green line) and right-shifted (dashed blue line) laser pulses in the center portion. For comparison, the center-enhanced laser pulse (solid red line) in case (a) is also shown. (d) Corresponding HHG power spectra for (c).

the norm of the field-free wave function is preserved to at least ten digits of accuracy during the time propagation. Having determined the time-dependent wave function $\psi(r,t)$, we can calculate the time-dependent induced dipole moment of the acceleration $d_A(t)$ and the HHG power spectrum.

First, we will focus on the relationship between the extension of the HHG cutoff and the generation of the shorter attosecond pulse. In Fig. 1(a), we show two laser fields. One is the fundamental 1064 nm laser pulse (dashed black line) and the other is the enhanced pulse (solid red line) in the center part, which is based on the 1064 nm laser pulse. The corresponding HHG power spectra from the hydrogen atom are shown in Fig. 1(b). We found that a single 240 as pulse can be obtained by superposing several harmonics near the cutoff regime for the fundamental 1064 nm laser pulse. However, an isolated and shorter 100 as pulse can be obtained for the laser pulse that is enhanced in the center part. In fact, we can see from Fig. 1(b) that there is a more extended and smoother supercontinuum plateau before the cutoff region for the enhanced-laser-field case. This broader and smooth supercontinuum plateau can be used to generate a shorter isolated attosecond pulse. In the following, we further explore the effect of modifying the pulse shape and see its consequence. We enhance the laser pulse in the center part to have a right shift (dashed blue line) or left shift (dotted green line), as shown in Fig. 1(c). It is interesting to note that the HHG supercontinuum plateau for the right-shifted case is from 80th to 120th order, significantly extending to 60 orders in the same peak-intensity laser, as shown in Fig 1(d). As a result, we can obtain an isolated and shorter 92 as pulse by superposing these broader supercontinuum harmonic spectra. Therefore, we know that the right-shift case is better than the center-enhanced or left-shift cases. Improving this method can produce the broader supercontinuum to obtain an increasingly shortened isolated attosecond pulse.

From the above discussion, we now consider how to find an optimized laser pulse which is enhanced and right shifted in the central part. Our proposed metrology can be realized by the two-color field with appropriate time delay between the two pulses. This two-color field $E_1(t)$ has the following form:

$$E_1(t) = A_1 f_1(t)\cos(\omega_1 t + \phi) + A_2 f_2(t-\tau)\cos(\omega_2 t - \tau). \tag{3}$$

As an example, $f_1(t)$ is the 5 fs Gaussian pulse with peak intensity $I_1 = 8 \times 10^{13}$ W/cm$^2$ and $f_2(t-\tau)$ is the 3 fs Gaussian pulse with peak intensity $I_2 = 4 \times 10^{14}$ W/cm$^2$. The time delay $\tau = 0.26\,T_1$ ($T_1 = \frac{2\pi}{\omega_1}$), frequencies $\omega_1 = 0.043$ a.u. ($\lambda_1 = 1064$ nm) and $\omega_2 = 0.0285$ a.u. ($\lambda_2 = 1600$ nm), carrier-envelope phase (CEP) $\phi = \frac{\pi}{2}$, and $A_1$ and $A_2$ are the corresponding electric field amplitudes. The time delay $\tau$ between the two pulses can control the steepness and height of the right-shifted peak. This laser field is presented in Fig. 2(a). In Fig. 2(b), we show the corresponding HHG power spectrum of hydrogen atoms driven by the optimized two-color laser

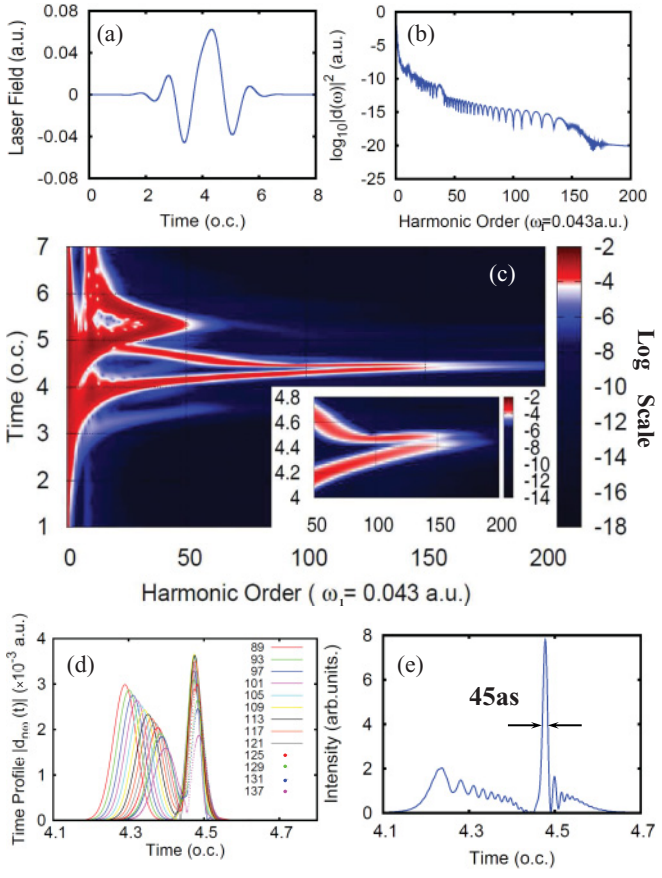


FIG. 2. (Color online) (a) Driving laser field $E_1(t)$ and (b) its HHG power spectrum for hydrogen atoms. (c) Wavelet time-frequency profile of HHG power spectra of hydrogen atoms driven by optimized two-color laser field and a detailed view (inset) of short and long trajectories near the cutoff. (d) Dipole time profiles of consecutive harmonics near cutoff. (e) Attosecond pulse produced by superposing the harmonics from 80th to 140th order.

field. We can see that there are two HHG plateaus. The cutoff of the first plateau is located at the 40th order. For the second plateau region, the HHG peaks are replaced by a series of pronounced supercontinua as separate adjacent peaks merge together, and the HHG cutoff is located at about the 150th order. The supercontinuum is from 50th to 140th order, extending 90 orders. According to the three-step model [17] of HHG, the cutoff energy of HHG is $I_p + 3.17U_p$, where $3.17U_p$ is the maximum energy of the quasifree electrons gained from the laser field. If only a 1064 nm fundamental laser field with the same intensity as the right-shifted two-color case is used, then the HHG cutoff will be at about the 45th order. That is to say, the HHG cutoff is extended about 100 harmonic orders by means of the optimized right-shifted two-color laser pulse. This is due to the fact that the electron experiences a longer acceleration time and can obtain more energy from the laser field when returning to the parent ion.

To figure out the detailed spectral and temporal time-dependent structures of HHG, we perform a time-frequency analysis by means of the wavelet transform of the induced dipole acceleration $d_A(t)$ [5],

$$A(t,\omega) = \int d_A(t')\sqrt{\omega}W(\omega(t'-t))dt' \equiv d_\omega(t). \qquad (4)$$

Here, $\omega$ is laser frequency and $W(\omega(t'-t))$ is the mother wavelet. Figure 2(c) shows the corresponding wavelet time-frequency profile of the HHG power spectra of hydrogen atoms driven by the optimized two-color laser field. Near the first cutoff region, starting from the 50th-order harmonic, we note that both the long- and short-trajectory electrons emit rapidly. The detailed view shows that the long-trajectory electrons emit in a shorter time range and contribute to each harmonic order near the second cutoff region. However, the short-trajectory electrons emit over a relatively longer time range. The corresponding time profiles of the consecutive harmonics from 89th to 137th harmonic order near the second cutoff region are shown in Fig. 2(d). It can be seen that each dipole time profile exhibits two peaks, which are generated by the broad and dispersive emission time of the short-trajectory electrons and by the relatively concentrated emission time of the long-trajectory electrons. Each emission-time burst agrees remarkably well with the time-frequency analysis shown in Fig. 2(c), and the contribution of the long trajectory dominates at the relatively short emission time compared with the short trajectory. Thus, it is possible to obtain a single attosecond pulse by superposing the harmonic spectra near the second cutoff region. The attosecond pulse $|W(t)|^2$ generated by the atom interacting with the laser field is calculated as

$$|W(t)|^2 = \left| \int_{\omega_i}^{\omega_f} d_A(\omega) \exp(-i\omega t) d\omega \right|^2. \qquad (5)$$

Here, $d_A(\omega)$ is the the Fourier transform of the induced dipole acceleration, and the supercontinuum in the HHG power spectrum begins from $\omega_i$ and extends to $\omega_f$. In Fig. 2(e), we show the generation of the attosecond pulse with the duration of 45 as can be obtained by superposing 60 orders of harmonics from the 80th to the 140th order. The reason for the generation such an isolated attosecond pulse can be understood as follows:

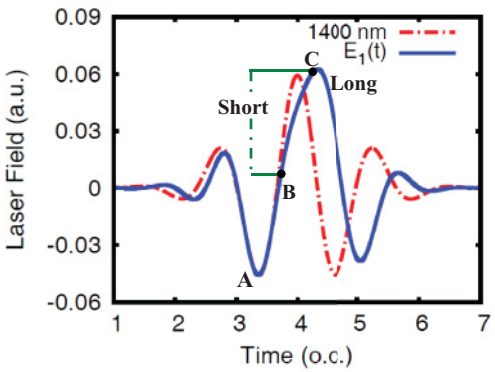


FIG. 3. (Color online) Red dashed line is laser field with peak intensity $I = 1.23 \times 10^{14}$ W/cm$^2$, wavelength $\lambda = 1400$ nm, and 5.26 fs Gaussian envelope. The blue line is the same as the optimized two-color laser field $E_1(t)$ shown in Fig. 2(a).

Figure 3 shows a 1400 nm laser field and the optimized two-color laser field [the same parameters are used as in Fig. 2(a)]. We choose the 1400 nm laser field to compare with the optimized two-color field because the duration and intensity of the main ionizing peak (marked by A) of this field is the same as the optimized two-color laser field. Generally speaking, long-trajectory electrons driven by the fundamental laser ionize earlier from peak A and return later to the nucleus and emit HHG spectra. On the other hand, short-trajectory electrons driven by the laser field ionize later and recombine earlier to the parent ion. For the present case, between 3.65 optical cycles (marked by B) and 4.1 optical cycles, the optimized two-color laser having lower intensity than that of the 1400 nm laser field delays the emission time of the electrons which are ionized from A. Furthermore, the optimized two-color field extends the short-trajectory duration from 3.65 optical cycles to 4.1 optical cycles and disperses the short-trajectory contribution, and long trajectory-electrons recombine to the nucleus after the mark C and produce congregating emission quickly for the successively climbing field. This optimized two-color laser field not only prolongs the short-trajectory electron emission time to depress the short-trajectory contribution, but also stimulates the abundant long-trajectory electrons to concentrate emission in 0.3 fs to produce an isolated 45 as pulse. Namely, we can get an isolated and short attosecond pulse by concentrating the emission time of the long-trajectory electrons near the cutoff region, and the emission time of the short-trajectory electrons is dispersed. As a result, we can obtain a shorter as laser pulse with a better contrast ratio, as will be further explored in Fig. 4.

While the 45 as pulse is produced by the previous optimized two-color field, the contrast ratio from the short-trajectory contribution is not small. To further optimize the two-color pulse, we now broaden and enhance the center part of the laser field more abundantly than the previous case. This revised laser field $E_2(t)$ has the same form as Eq. (3), where $f_1(t)$ is now the 5 fs Gaussian pulse with peak intensity $I_1 = 2 \times 10^{13}$ W/cm$^2$ and $f_2(t-\tau)$ is the 5 fs Gaussian pulse with peak intensity $I_2 = 5 \times 10^{14}$ W/cm$^2$. The time delay is $\tau = -0.28T_1$, frequencies $\omega_1 = 0.057$ a.u. ($\lambda = 800$ nm) and $\omega_2 = 0.0228$ a.u. ($\lambda_2 = 2000$ nm), and the CEP $\phi = \pi$. Note

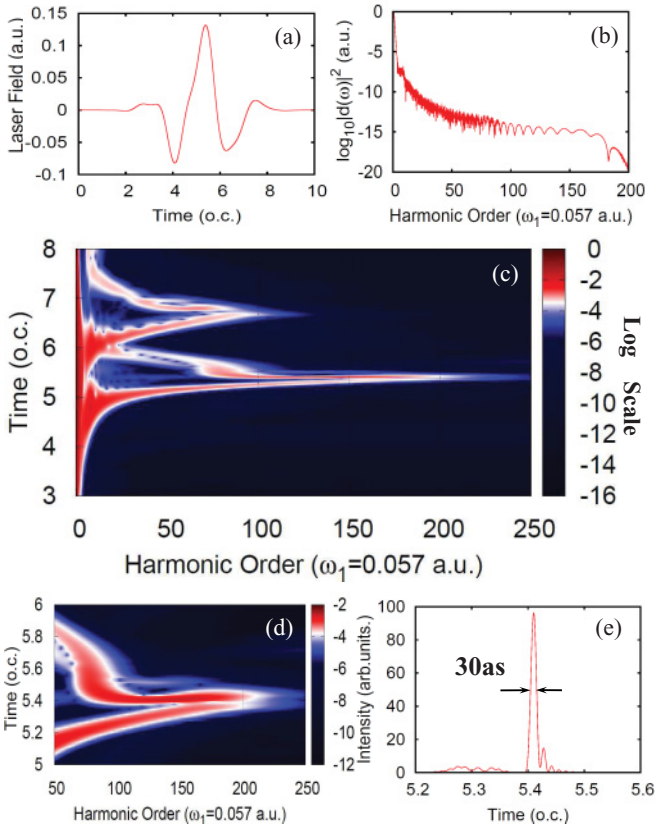


FIG. 4. (Color online) (a) Driving laser field $E_2(t)$ and (b) its HHG power spectrum for hydrogen atoms. (c) Wavelet time-frequency profile of the HHG power spectra of hydrogen atoms driven by the optimized laser field and (d) a more detailed view of the dipole time profiles of the short trajectory (weak intensity) and long trajectory (higher intensity). (e) Corresponding isolated attosecond pulse produced by superposing the harmonics from the 93rd to 175th order.

that an optical parametric amplifier laser system can provide 2000 nm high-intensity laser light [19]. The hollow-fiber pulse compressor device can be used to compress the multi-mJ pulse down to the few-cycle pulse regime [20].

The optimized laser pulse is depicted in Fig. 4(a). Figure 4(b) shows the corresponding HHG power spectrum of hydrogen atoms driven by this optimized two-color laser field. Figure 4(c) shows the wavelet time-frequency profile, which indicates the existence of a narrow long-trajectory burst with strong intensity from the 93rd to 175th harmonics. In the previous 45-as-pulse case, we note that the long-trajectory intensity is about the same order as that of the short-trajectory intensity. However, from Fig. 4(d), we can see clearly that there is an enhancement of the long-trajectory emission contribution before the cutoff region, and the short-trajectory emission is weak. Quasifree electrons are accelerated more strongly by this broader and enhanced field $E_2(t)$. The emission time of the short-trajectory electrons is prolonged longer and longer, and the short-trajectory contribution to each harmonic is dispersed to a relatively longer time period. On the other hand, the long-trajectory electron emission is focused in a specifically narrower duration. In other words, using this method not only generates a narrow attosecond pulse by long-trajectory emission, but also decreases the contrast ratio caused by the short-trajectory emission. We can suppress the short trajectory to purify the attosecond pulse by this optimized two-color laser field. Figure 4(e) shows an example. We superpose the 93rd to 175th order harmonics, leading to the generation of an isolated 30 as pulse with a bandwidth of 127 eV. We believe that this proposed metrology can be extended to other systems and can provide an efficient method for the production of isolated ultrashort attosecond pulses for the future.

This work was partially supported by the Chemical Sciences, Geosciences, and Biosciences Division of the Office of Basic Energy Sciences, Office of Sciences, US Department of Energy and by the US National Science Foundation. We also would like to acknowledge the partial support of the National Science Council of Taiwan (Grant No. 100-2119-M-002-013-MY3) and the National Taiwan University (Grant No. 10R80700). PCL acknowledges the partial support of the National Natural Science Foundation of China (Grant Nos. 11044007 and 11047016), and the Young Teachers Foundation of the Northwest Normal University (NWNU-LKQN-10-5).

[1] P. B. Corkum and F. Krausz, Nat. Phys. **3**, 381 (2007).
[2] F. Krausz and M. Ivanov, Rev. Mod. Phys. **81**, 163 (2009).
[3] M. Hentschel *et al.*, Nature (London) **414**, 509 (2001).
[4] A. Baltuška *et al.*, Nature (London) **421**, 611 (2003).
[5] J. J. Carrera, X. M. Tong, and S. I. Chu, Phys. Rev. A **74**, 023404 (2006).
[6] R. Kienberger *et al.*, Science **297**, 1144 (2002).
[7] S. Baker *et al.*, Science **312**, 424 (2006).
[8] M. Uiberacker *et al.*, Nature (London) **446**, 627 (2007).
[9] M. Drescher *et al.*, Nature (London) **419**, 803 (2002).
[10] J. Itatani *et al.*, Nature (London) **432**, 867 (2004).
[11] P. H. Bucksbaum, Science **317**, 766 (2007).
[12] E. Goulielmakis *et al.*, Nature (London) **436**, 739 (2010).
[13] H. Mashiko *et al.*, Opt. Lett. **34**, 3337 (2009).
[14] E. Goulielmarkis *et al.*, Science **320**, 1614 (2008).
[15] T. Siegel *et al.*, Opt. Express **18**, 7 (2010).
[16] Leonardo Brugnera *et al.*, Opt. Lett. **35**, 3994 (2010).
[17] P. B. Corkum, Phys. Rev. Lett. **71**, 1994 (1993).
[18] X. M. Tong and S. I. Chu, Chem. Phys. **217**, 119 (1997).
[19] C. I. Blaga *et al.*, Nat. Phys. **5**, 335 (2009).
[20] X. Chen *et al.*, Appl. Phys. B **99**, 149 (2010).